(2)

MTL TR 89-93 **AD-A215 172** AD

FRACTOGRAPHIC ANALYSIS OF LONG ROD PENETRATOR-ARMOR CERAMIC INTERACTIONS

MICHAEL J. SLAVIN
CERAMICS RESEARCH BRANCH

October 1989

Approved for public release; distribution unlimited.

US ARMY
LABORATORY COMMAND
MATERIALS TECHNOLOGY LABORATORY

U.S. ARMY MATERIALS TECHNOLOGY LABORATORY
Watertown, Massachusetts 02172-0001

The findings in this report are not to be construed as an official Department of the Army position, unless so designated by other authorized documents.

Mention of any trade names or manufacturers in this report shall not be construed as advertising nor as an official indorsement or approval of such products or companies by the United States Government.

DISPOSITION INSTRUCTIONS

Destroy this report when it is no longer needed.
Do not return it to the originator

UNCLASSIFIED

SECURITY CLASSIFICATION OF THIS PAGE (When Data Entered)

REPORT DOCUMENTATION PAGE		READ INSTRUCTIONS BEFORE COMPLETING FORM
1. REPORT NUMBER MTL TR 89-93	2. GOVT ACCESSION NO	3. RECIPIENT'S CATALOG NUMBER
4. TITLE (and Subtitle) FRACTOGRAPHIC ANALYSIS OF LONG ROD PENETRATOR-ARMOR CERAMIC INTERACTIONS		5. TYPE OF REPORT & PERIOD COVERED Final Report 6. PERFORMING ORG. REPORT NUMBER
7. AUTHOR(s) Michael J. Slavin		8. CONTRACT OR GRANT NUMBER(s)
9. PERFORMING ORGANIZATION NAME AND ADDRESS U.S. Army Materials Technology Laboratory Watertown, Massachusetts 02172-0001 SLCMT-EMC		10. PROGRAM ELEMENT, PROJECT, TASK AREA & WORK UNIT NUMBERS D/A Project: 1L162105.AH84
11. CONTROLLING OFFICE NAME AND ADDRESS U.S. Army Laboratory Command 2800 Powder Mill Road Adelphi, Maryland 20783-1145		12. REPORT DATE October 1989 13. NUMBER OF PAGES 15
14. MONITORING AGENCY NAME & ADDRESS (if different from Controlling Office)		15. SECURITY CLASS (of this report) Unclassified 15a. DECLASSIFICATION/DOWNGRADING SCHEDULE

16. DISTRIBUTION STATEMENT (of this Report)

Approved for public release; distribution unlimited.

17. DISTRIBUTION STATEMENT (of the abstract entered in Block 20, if different from Report)

18. SUPPLEMENTARY NOTES

Presented at the 5th TACOM Armor Coordinating Conference Proceedings, 7-9 March 1989.

19. KEY WORDS (Continue on reverse side if necessary and identify by block number)

Armor	Ballistic performance
Ceramic armor	Fracture (mechanics)
Long rod penetrators	Scanning electron microscopy

20. ABSTRACT (Continue on reverse side if necessary and identify by block number)

(SEE REVERSE SIDE)

DD FORM 1 JAN 73 1473 EDITION OF 1 NOV 65 IS OBSOLETE

UNCLASSIFIED

SECURITY CLASSIFICATION OF THIS PAGE (When Data Entered)

Block No. 20

ABSTRACT

The stages of armor ceramic fracture and defeat mechanisms of the projectile have been well documented for small caliber rounds (.30 and .50 caliber ball and armor piercing). The recent ability to manufacture ceramic tiles capable of protecting vehicles against large caliber munitions has shifted research to incorporating these materials into ground systems. Though many studies are evaluating the relationship of processing, microstructure, and mechanical properties with ballistic performance, few programs have focused on the actual defeat mechanisms involved for these heavy threats.

A program was initiated to evaluate the fracture of a ceramic target when impacted by a tungsten long-rod penetrator (LRP). Following a conventional V_{50} test of a silicon carbide whisker-reinforced aluminum oxide, one target was serial sectioned from the rear. Very fine comminuted ceramic was painstakingly removed from the exit point of the LRP. Tungsten and steel particles were included in the ceramic powder. The steel was present from three sources: front plate penetration, back plate splash, and subsequent entry into the target of the pusher plate. A distinct transition from very fine ceramic rubble to large ceramic pieces with a boundary geometry identical to that of a fracture conoid was apparent.

All metallic material uncovered was removed for fractographic evaluation. The tungsten particles had comminuted ceramic embedded in it. This fractured ceramic would have been subjected to the maximum stresses from the ballistic impact and would give specific details as to the fracture mode of the ceramic directly in front of the projectile. Scanning electron microscopy (SEM) showed that the defeat mechanisms of the LRP were ductile tearing and microerosion by the very fine comminuted ceramic. Both the alumina grains and silicon carbide whiskers showed signs of mixed failure modes (transgranular and intergranular).

CONTENTS

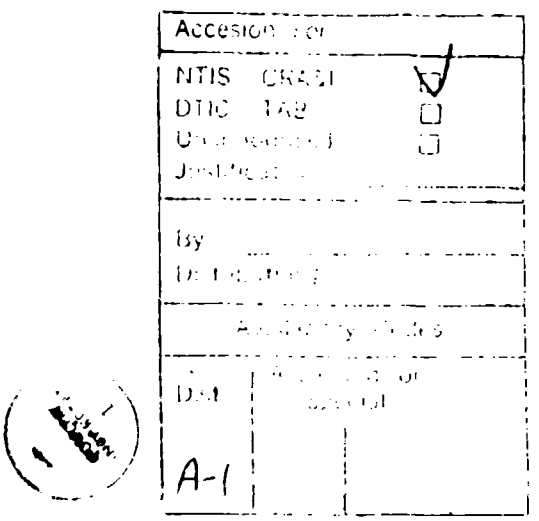

INTRODUCTION

Research efforts evaluating the ballistic capabilities of ceramic materials have typically focused on empirical methods of ranking performance versus a specific threat.[1-5] More recently, experimentalists have begun looking at processing, microstructure, and the resulting mechanical properties, and how they relate to the ballistic performance.*,[1,6-8] Only a few studies have concentrated on the projectile-armor interactions and the resulting fracture.[9-12]

Previous fractographic examination of ballistic rubble[12] concentrated solely on random samples of the comminuted ceramic removed from the penetration area immediately following the test event. While this revealed useful information regarding the fracture mode and morphology of the ceramic, it yielded no data on the ceramic-penetrator interactions. Recent efforts have focused on careful material removal of all metallic particulates remaining in the target following a typical ballistic test.

EXPERIMENTAL PROCEDURE

As part of a conventional V_{50} test sequence, an armor target was recovered and held for careful autopsy. The quarterscale ballistic test configuration consisted of: a 97 weight-percent tungsten (97 W) long-rod penetrator with an aspect ratio of 10 (L/D = 10) and a laminate armor package consisting of steel ESR 4340 (HRC = 52 to 55) front and back plates of thicknesses 0.63 and 1.90 cm, respectively, sandwiching a ceramic tile 2.54 cm thick, as shown in Figure 1. The 15.24- x 15.24- x 5.08-cm target was rigidly clamped together with moderate lateral constraint. The ceramic being evaluated was a 30 volume-percent silicon carbide (SiC) whisker-reinforced aluminum oxide.*,[6]

The last of six targets, retained intact following the ballistic testing, was carefully moved so as not to disturb the comminuted material. The ESR 4340 back plate was removed from the target and the comminuted ceramic was meticulously excavated from the exit area of the penetrator. As the ceramic was removed from this area, new ceramic continually tumbled into the site. All metallic particles found during serial sectioning of the target were retained along with random samples of ceramic. Photographs were taken at constant mass intervals of particulate removal to document the serial sectioning of the target (see the Appendix).

*SLAVIN, M. J., VIECHNICKI, D. J., and TRACY, C. A. *Processing, Microstructure and Property Relationships of Armor Ceramics.* To be published in Proceedings of 1988 U.S. Army Science Conference, October 1988.

1. WILKINS, M. L., HONODEL, C., and SAWLE, D. *An Approach to the Study of Light Armor.* Lawrence Radiation Laboratory, University of California, Livermore, CA, UCRL-50284, 1967.
2. WILKINS, M. L., CLINE, C. F., and HONODEL, C. A. *Fourth Progress Report of Light Armor Program.* Lawrence Radiation Laboratory, University of California, Livermore, CA, UCRL-50694, 1969.
3. LANDINGHAM, R. L., and CASEY, A. W. *Semiannual Progress Report of the Light Armor Materials Program.* Lawrence Radiation Laboratory, University of California, Livermore, CA, UCRL-510665, 1971.
4. LANDINGHAM, R. L., and CASEY, A. W. *Final Report of the Light Armor Materials Program.* Lawrence Radiation Laboratory, University of California, Livermore, CA, UCRL-512695, 1972.
5. MASCIANICA, F. S. *Ballistic Technology of Lightweight Armor - 1981.* U.S. Army Materials Technology Laboratory, AMMRC TR 81-20 (Secret).
6. VIECHNICKI, D., BLUMENTHAL, W., SLAVIN, M., TRACY, C., and SKEELE, H. *Armor Ceramics - 1987* in Proceedings of the Third Annual TACOM Armor Coordinating Conference, 1987.
7. ZUKAS, J. A., NICHOLAS, T., SWIFT, H. F., GRESZCZUK, L. B., and CURRAN, D. R. Impact Dynamics. John Wiley & Sons, New York, 1982.
8. ROZENBERG, Z., and YESHURUN, Y. *The Relationship Between Ballistic Efficiency and Compressive Strength of Ceramic Tiles.* Int. J. Impact Engng., v. 7, no. 3, 1988, p. 357-362.
9. FRECHETTE, V. D., and CLINE, C. F. *Fractography of Ballistically Tested Ceramics.* J. Am. Ceram. Soc., v. 49, no. 11, 1970, p. 994-997.
10. KATZ, R. N., and BRANTLEY, W. A. *Fractography of High Boron Ceramics Subjected to Ballistic Loading* in Materials Science Research, W. W. Kriegel, ed., Plenum Press, New York, v. 5, 1971, p. 271-282.
11. HORNEMANN, U., ROTHENHAUSLER, H., SENF, H., KALTOFF, J. F., and WINKLER, S. *Experimental Investigation of Wave and Fracture Propagation in Glass Slabs by Steel Cylinders at High Impact Velocities* in Mechanical Properties at High Rates of Strain, J. Harding, ed., Conference Series No. 70, The Institute of Physics, Bristol and London, 1984, p. 291.
12. TRACY, C., SLAVIN, M., and VIECHNICKI, D. *Ceramic Fracture During Ballistic Impact* in Advances in Ceramics: Fractography of Glasses and Ceramics, The American Ceramic Society, Ohio, v. 22, 1988, p. 295-306.

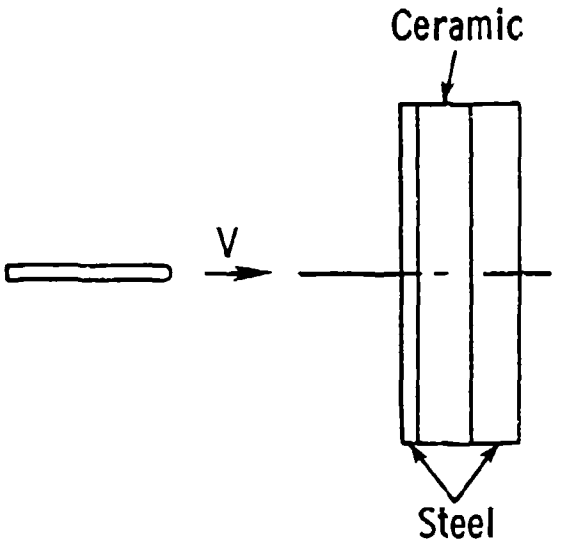

Figure 1. Schematic showing the penetrator and target configuration.

The tungsten and steel particles were separated using a small magnet. A range of particle sizes were chosen for detailed microscopy. Approximately one-half of each set of particles was then ultrasonically cleaned to provide an unobstructed view of the particles with the balance retained to show the ceramic-penetrator interactions, as well as a more precise view of the fractured ceramic that defeats the penetrator. Both sets of particulates were then viewed in a scanning electron microscope.* Electron dispersive spectroscopy (EDS) was employed to determine the elements present in any sample.

RESULTS AND DISCUSSION

Photomicrographs of polished sections of the penetrator and armor ceramic are shown in Figure 2. The tungsten has a very uniform and homogeneous microstructure with an average grain size of approximately 80 μm. The alumina phase of the composite has an average grain size of approximately 2 μm with scattered agglomerates of 10 to 15 μm grains surrounded by whiskers. The SiC whiskers, <1 μm in diameter with aspect ratios up to 20, are well dispersed in the matrix, except for the agglomerate sites, but have a preferred orientation in the plane of the tile (perpendicular to the penetration direction).

The sixth target in the V_{50} evaluation was impacted at a velocity in excess of 1 km/sec at 0° obliquity and was a complete penetration. The residual stub of the penetrator was inadvertently not recovered. The material removed from the rear of the target was collected, however little attention was given to the location of the metallic particles since shifting during movement may have diminished the likelihood of obtaining useful data.

A significant amount of both the steel and penetrator particles were recovered from the target, but not enough to account for the total mass removed during penetration. During the initial impact into the target, various particles of steel indicated that the front plate melted,

*Jeol Model JXA-840, Tokyo, Japan.

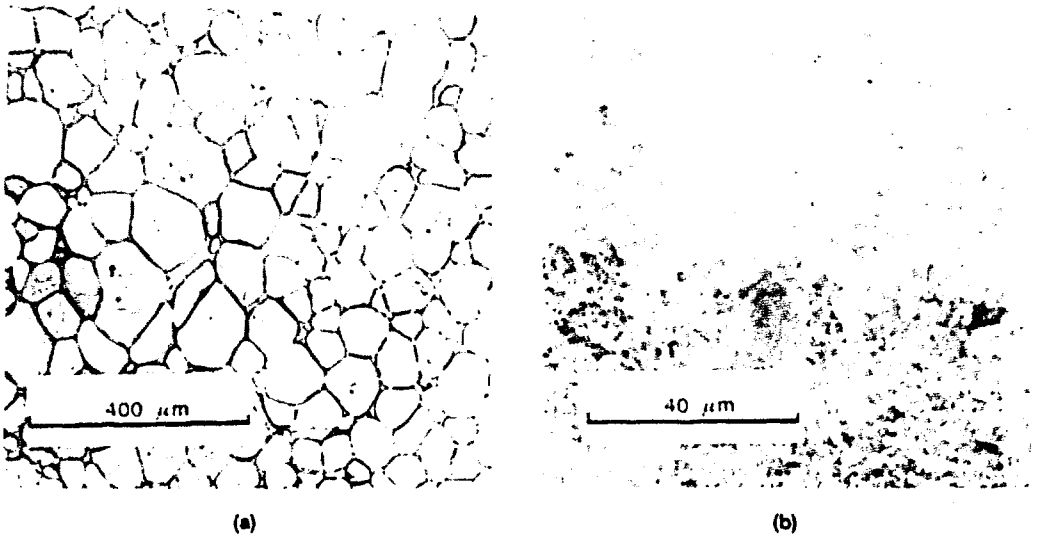

Figure 2. Polished sections of (a) the 97% tungsten penetrator and (b) the aluminum oxide with silicon carbide whiskers.

as shown in Figure 3. Highly deformed tungsten grains are also produced, however, it is very likely that the penetrator is continually deformed plastically at the projectile-target interface throughout the penetration, as shown in Figure 4.

As the tungsten projectile penetrates into the ceramic portion of the target, it encounters material that has been subjected to shock waves of very high magnitude. Previous work indicates that the ceramic may begin to fracture due to the compressive stress developed from the initial impact and resultant shock wave.[11,13] Compressive fracture theory[14] suggests that microcracks will initiate and propagate from all flaws properly oriented to the compressive field. This type of failure would produce a large quantity and size distribution of comminuted ceramic in the region of maximum compressive stress, as shown in Figure 5.

The composite ceramic displayed a mixed fracture mode. The alumina matrix failed transgranularly and intergranularly. The SiC whiskers caused crack deflection at the matrix-whisker interface, as shown in Figure 6. The composite ceramic was processed with less than 0.1 weight-percent magnesia as a grain-growth inhibitor and is otherwise free of impurities and grain boundary phases. The effect of microstructure versus the mode of fracture and toughening mechanism has been previously addressed.[6,12]

As time elapses, destructive tensile stresses generated by the release waves will cause more global failure of the ceramic tile (see the Appendix, Figure A-1, photograph nos. 13 and 14). These tensile failures will initiate when release waves pass the existing flaws in the ceramic, i.e., agglomerates of large alumina grains surrounded by SiC whiskers, and when the tile experiences bending stresses. Tensile fracture of ceramics has been well addressed in the literature and is based on the work by Griffith.[15]

13. MESCALL, J. F., and TRACY, C. A. *Improved Modeling of Fracture in Ceramic Armor.* Proceedings of the 1986 U.S. Army Science Conference, June 1986.
14. SINES, G., and ADAMS, M. *A Statistical Micromechanical Theory of the Compressive Strength of Brittle Materials.* J. Am. Ceram. Soc., v. 60, no. 3-4, 1978, p. 126-131.
15. GRIFFITH, A. A. in Proceedings of the 1st International Congress for Applied Mechanics. S. B. Biezeno and J. M. Burgers, ed., Walatman Uitgeverij, Delft, The Netherlands, 1924, p. 55-63.

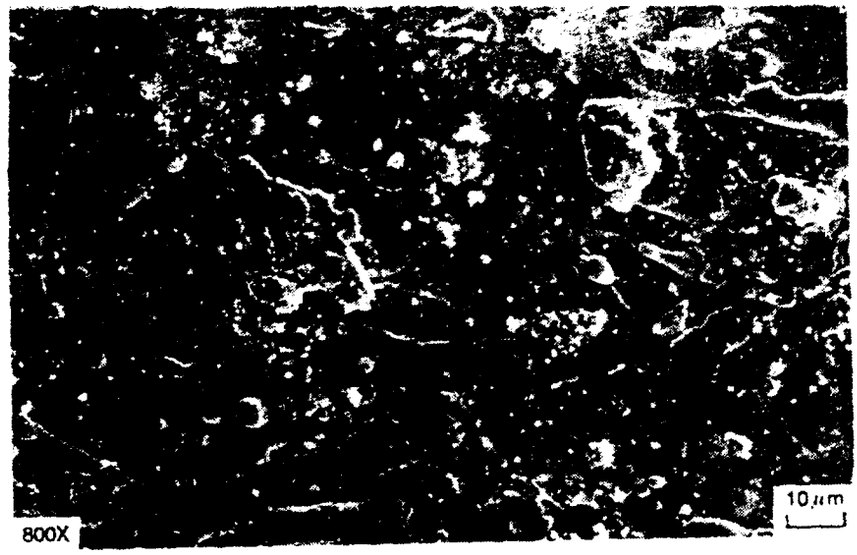

(a)

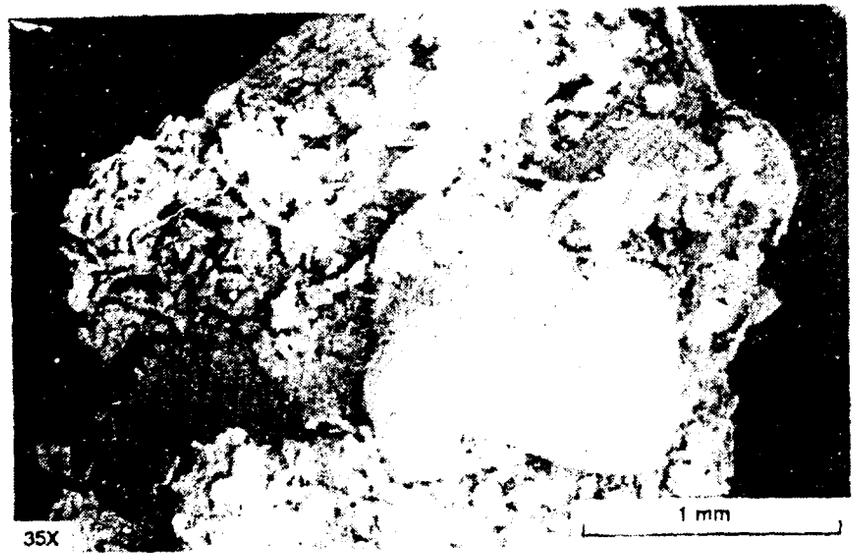

(b)

Figure 3. Steel particles showing (a) resolidified surface and (b) embedded plastically deformed tungsten.

The tungsten penetrator encounters highly confined, comminuted ceramic as it enters the center of the target. The penetrator traveling into the much harder ceramic will be similar to the abrasive process of a grinding wheel acting on a metallic workpiece since the ceramic will exert a large force on the nose and the lateral surfaces of the projectile. This abrasive process is divided into two basic mechanisms: cutting and ploughing of the workpiece.[16]

16. ABEBE, M., and APPL, F. C. *Theoretical Analysis of the Basic Mechanics of Abrasive Processes, Part I: General Model.* Wear, v. 126, no. 3, 1988, p. 251-266.

Cutting consists of material removal along with some plastic flow to the sides of the grit, while ploughing results only in plastic deformation to the sides and beneath the grit. The transition from cutting to ploughing is a function of the grit geometry and the angle that it impinges the piece. Both cutting and ploughing of the tungsten are clearly evident on many of the particles examined, as shown in Figures 7 and 8.

Figure 4. Plastically deformed tungsten grains at the edge of a recovered particle.

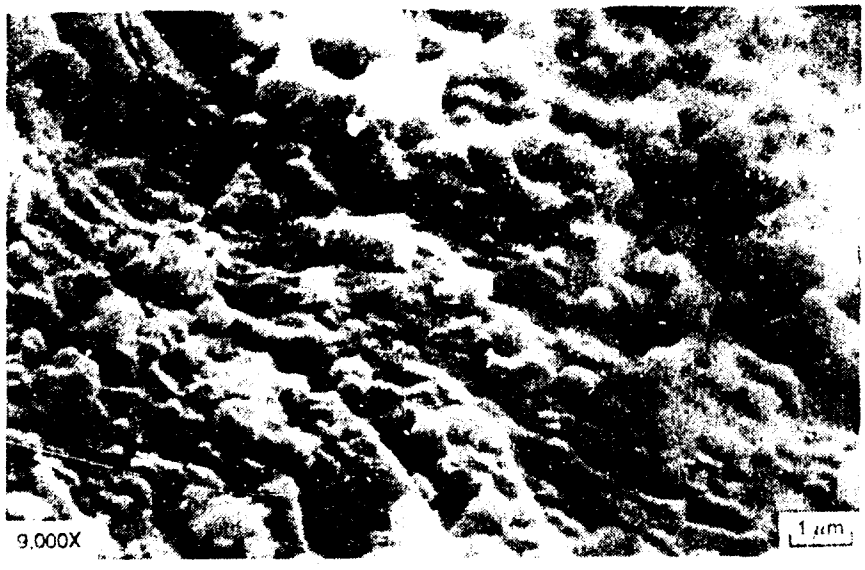

Figure 5. Comminuted ceramic embedded on the surface of a tungsten particle. Note the size range of the alumina particles and SiC whiskers.

Figure 6. Larger particle showing the mixed fracture mode, transgranular and intergranular, of the composite ceramic. Note the crack deflection by the SiC whisker.

The size and geometry of the comminuted ceramic will stay relatively constant after it is fractured by the various shock waves. Only interactions with other ceramic particulates will cause further fracture; therefore, only the angle of impingement will change during penetration as the comminuted ceramic tumbles, or "flows," around the projectile as it penetrates the target.

The confinement force and the size of the comminuted ceramic are very important in the abrasive process. As the size decreases, the ceramic's ability to flow will increase. If the shape of the comminuted ceramic is very regular, or residual porosity is present in the bulk ceramic that would collapse after comminution, then flow will be enhanced. Lubrication of the particulates from possible melting of grain boundary phases will increase the ceramic's flow rate. Metallic and glass grain boundaries would be prone to this occurrence if the temperature is increased locally during penetration. As the flowability increases in the ceramic, the confining force in the target will be reduced and will decrease the material removed from the penetrator by decreasing the depth and the length of the abrasive cuts.

The presence of a large scale failure mechanism, aside from plastic deformation, that would contribute to the defeat of the penetrator would be advantageous. Removal of large pieces of tungsten would quickly reduce the momentum and kinetic energy of the penetrator. Figures 9 and 10 show a tungsten particle that, in addition to being abrasively eroded, has been subjected to large scale crack propagation, or tearing, that has produced an intergranular surface. For the surface to be in such a pristine condition, the comminuted ceramic would either be in a relatively rigid or unconfined state since there is more than sufficient clearance for the comminuted ceramic to enter and abrade the surface. These conditions would be present early in the penetration of the ceramic, or later in the process after the penetrator has passed and the ceramic is beginning to release and collapse.

Enhancement of tearing of the projectile may be possible by the incorporation of a well-dispersed, bimodal grain-size distribution in the monolithic ceramic or the addition of a second, hard phase in the matrix. Both cases would benefit from a sharp grit geometry. The agglomerates of large alumina grains (only 10 to 15 μm) are probably too small to cause tearing.

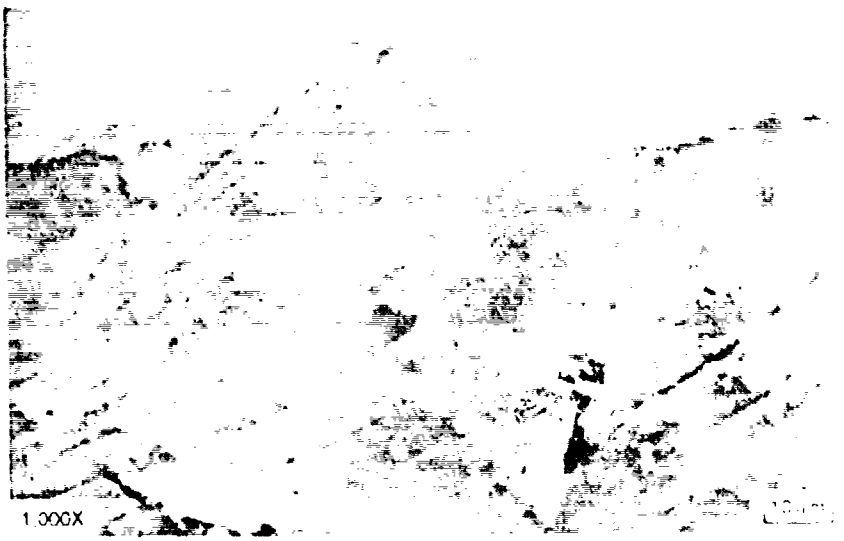

Figure 7. Surface of a tungsten particle that has been abraded by comminuted ceramic which is still present. Note the plastic deformation at the grain boundaries.

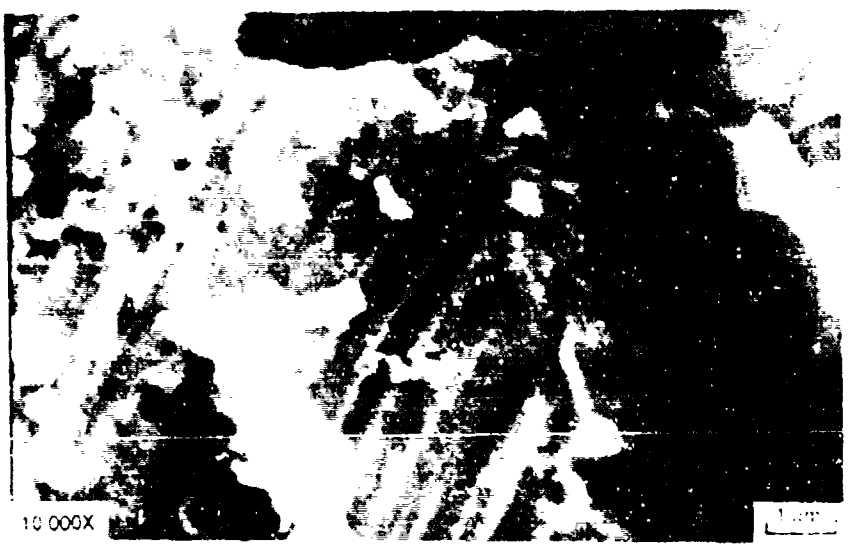

Figure 8. Closeup of surface of a tungsten particle with comminuted ceramic of similar size to the depth of the cut grooves.

Figure 9. Tungsten particle with both abrasive grooves and exposed grains, possibly produced by ductile tearing.

CONCLUSIONS

The steel front plate shows signs of melting indicating that there are high temperatures generated at least during the initial stages of the penetration event. The initial impact also produces a large amount of plastic deformation in the tungsten penetrator. Grains which were nearly spherical are tabular after impact.

The composite ceramic failed in a mixed fracture mode in the path of the penetrator (transgranular and intergranular). Much of the comminuted ceramic still embedded in the penetrator fragments are smaller than the original grain size of the ceramic. The addition of the SiC whiskers increased the fracture toughness over that of a monolithic alumina by crack deflection at the whisker-matrix interface.

Microerosion due to abrasion by the comminuted ceramic seems to be the prime material removal mechanism of the penetrator, however, ductile tearing has the potential for removing larger pieces. Increases in the abrasive process may be possible by producing the very irregular and sharp "grit" that can cut into the more ductile penetrator. This would be accomplished by promoting transgranular fracture of the ceramic. An intergranular fracture would produce a more regular-shaped particle which would plough (plastic deformation) but not cut the tungsten.

Increasing the larger scale ductile tearing of the penetrator would expose new surface area that would be further subject to abrasion. This could be accomplished by incorporating a bimodal grain-size distribution into the monolithic ceramic, or by adding a second phase particulate/grit of a harder material. The purpose of this addition would not necessarily be to increase the fracture toughness of the ceramic and dissipate more energy by the creation of free surfaces, but to directly decrease the momentum and kinetic energy of the penetrator.

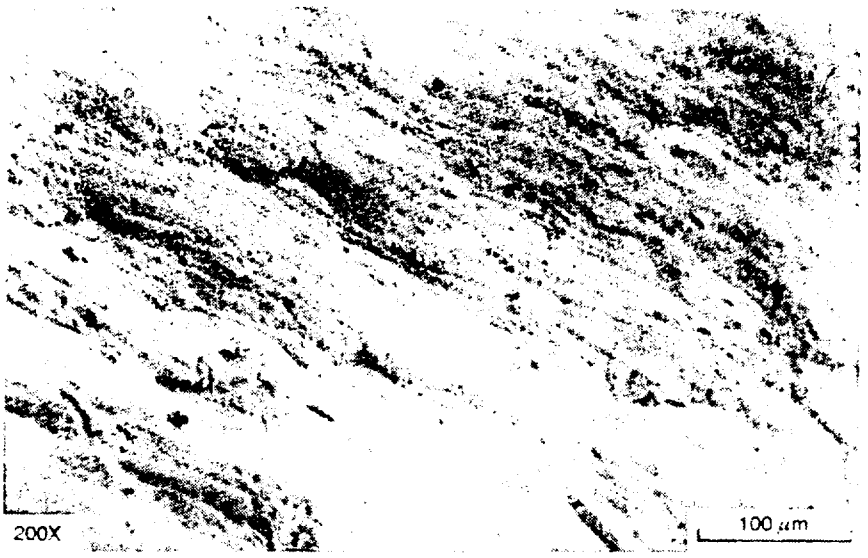

(a)

(b)

Figure 10. Higher magnification of both surfaces shown in Figure 9. Note the difference of scale between (a) the barely distinguishable groovos and (b) the tungsten grains with no abrasion.

Since an abrasive material removal process seems to be dominant in the defeat of the penetrator, it is essential to keep a high confining force on the ceramic and penetrator and reduce the ceramic's ability to flow. If temperatures near the ceramic-projectile interface are elevated throughout the penetration event, it would be prudent not to have either a metallic or glassy grain boundary phase that could melt and "lubricate" the comminuted ceramic. Grain boundary phases tend to shift the fracture mode of the ceramic to intergranular which

produces a more regularly shaped particle. Both scenarios would increase the flowability of the ceramic, decrease the confining force between the comminuted ceramic and projectile, and reduce the material removal rate due to abrasion.

Postballistic fractography, though not as useful as direct observation of the fracture during the ballistic event, is relatively straightforward and simple to carry out. Other armor ceramics will be evaluated to determine the fracture and erosion characteristics, with respect to the microstructure, of a ballistic event and may shed light on whether microstructure tailoring can improve the abrasive behavior and ballistic performance.

ACKNOWLEDGMENTS

The author wishes to thank Messrs. Philip Vincent, David Kokidko, and John Segalla for their efforts in performing the ballistic tests and their patience with the author in collecting fractured ceramic immediately following the test. The author also wishes to thank Ms. Gail Meyers for her hours spent looking at fracture surfaces of ceramic, tungsten, and steel with the scanning electron microscope.

APPENDIX.

Shown in Figure A-1 are photographs taken during the serial section of the armor target. These photographs are looking at the rear of the target after initial removal of the 3/4-inch back plate to the final removal of all the loose fractured ceramic. Only 8 of 14 sections are shown here due to space requirements. The section photograph number is in parentheses. (Tile size is 6 x 6 inches.)

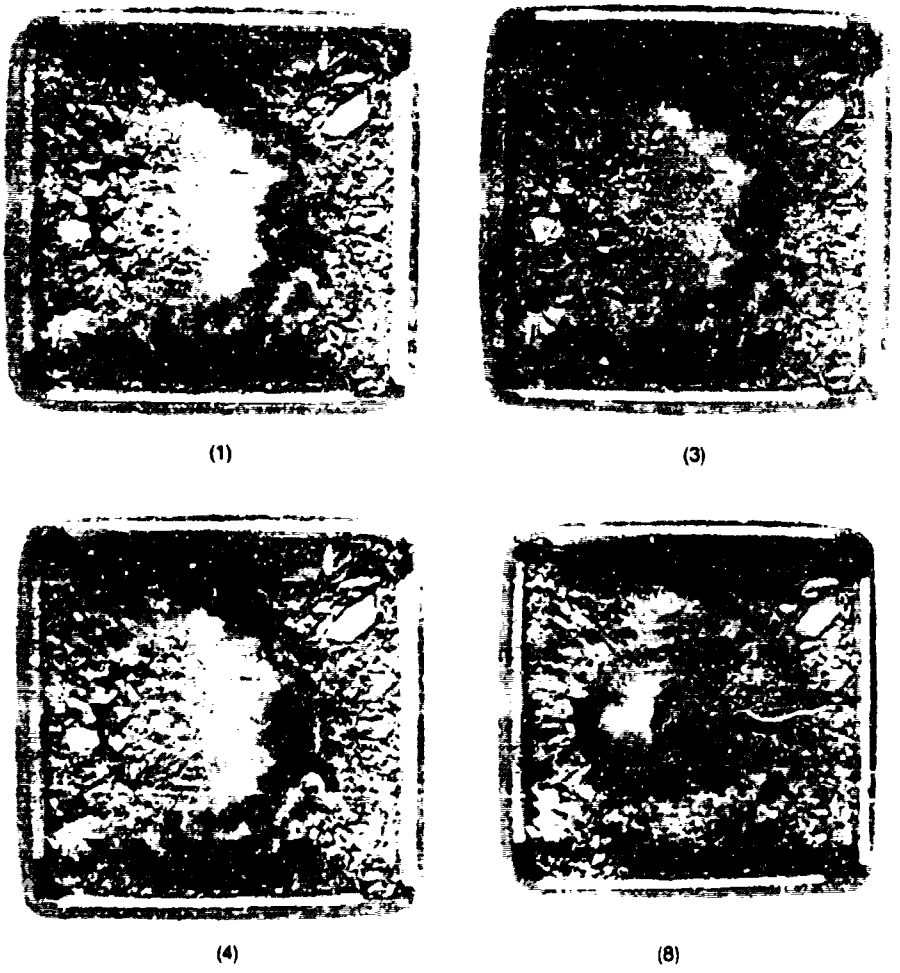

Figure A-1. Section photograph (1) shows the relatively large area of finely comminuted ceramic (approximately 4 inches in diameter) present at the rear of the tile. Since a fractured and unconfined ceramic cannot support a tensile stress wave, the comminuted ceramic fractured to such an extent due to compressive and/or shear stresses during penetration as the ceramic "flows" around the penetrator. Section photographs (3), (4), and (8) give an indication of the volume and distribution of comminuted ceramic in a cone toward the point of entrance of the penetrator.

(10)

(12)

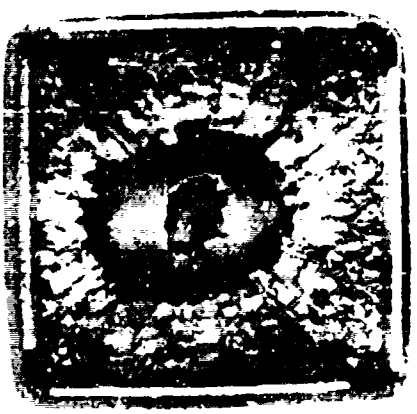

(13)

(14)

Figure A-1 (cont'd). Photos (10), (12), and (13) depict the transition from the heavily fractured ceramic to larger fragments caused by radial (bending) and conical (hertzian) cracking. The large and irregular hole in the steel cover plate is due to the projectile penetration and ejecta of comminuted ceramic during ballistic event. The exit hole in the rear plate (not shown) had a splash of approximately 3/4 inch in diameter and a final diameter of less than 1/2 inch. Section photo (14) shows the tile with all loose fragments removed. The radial fracture seems to be the primary crack system for the region near the front, exterior of the tile. These fragments were very difficult to remove due to the lateral confinement of the tile.

DISTRIBUTION LIST

No. of Copies	To
	Office of the Under Secretary of Defense for Research and Engineering, The Pentagon, Washington, DC 20301
1	ATTN: Mr. J. Persh
1	Dr. W. E. Snowden
	Director, Defense Advanced Research Project Agency, 1400 Wilson Boulevard, Arlington, VA 22901
1	ATTN: LTC P. H. Sullivan
1	Dr. J. Richardson
1	Dr. B. Wilcox
1	LTC D. Wance
	Commander, U.S. Army Laboratory Command, 2800 Powder Mill Road, Adelphi, MD 20783-1145
2	ATTN: AMSLC-IM-TL, Mr. R. Vitali
1	AMSLC-CT
	Commander, Defense Technical Information Center, Cameron Station, Bldg. 5, 5010 Duke Street, Alexandria, VA 22304-6145
2	ATTN: DTIC-FDAC
1	Metals and Ceramics Information Center, Battelle Columbus Laboratories, 505 King Avenue, Columbus, OH 43201
	Commander, Army Research Office, P.O. Box 12211, Research Triangle Park, NC 27709-2211
1	ATTN: Information Processing Office
1	SLCRO-MD, Dr. I. Ahmad
	Commander, U.S. Army Materiel Command, 5001 Eisenhower Ave. Alexandria, VA 22333
1	ATTN: AMCLD
1	AMCDE-SR, Dr. R. Chait
1	Mr. R. Zigler
	Commander, U.S. Army Materiel Systems Analysis Activity, Aberdeen Proving Ground, MD 21005
1	ATTN: AMXSY-MP, H. Cohen
	Commander, U.S. Army Missile Command, Redstone Scientific Information Center, Redstone Arsenal, AL 35898-5241
1	ATTN: AMSMI-RD-CS-R/Doc
1	AMSMI-RLM
	Commander, U.S. Armament, Munitions and Chemical Command, Dover, NJ 07801
2	ATTN: Technical Library
1	AMDAR-LCA, Mr. Harry E. Pebly, Jr., PLASTEC, Director
	Commander, U.S. Army Natick Research, Development and Engineering Center, Natick, MA 01760
1	ATTN: Technical Library
1	Dr. R. Lewis
	Commander, U.S. Army Tank-Automotive Command, Warren, MI 48397-5000
2	ATTN: AMSTA-TSL, Technical Library
1	AMSTA-ZSK
1	AMSTA-RSK, Sam Goodman
1	AMSTA-RSK, David Tenenbaum
1	AMSTA-RSK, Dr. James L. Thompson
1	AMCPM-M113-T, G. B. Singh
1	AMCPM-M113, Mr. Joseph Loiselle
1	AMCPM-BFVS, Gary Chamberlain
	Commander, U.S. Army Materials Systems Analysis Activity, Aberdeen Proving Ground, MD 21005-5071
1	ATTN: AMXSY-GI, James Liu
1	AMXSY-GI, Gary Holloway
	Commander, Combat Systems Test Activity, Aberdeen Proving Ground, MD 21005-5059
2	ATTN: STECS-AA-R, Roy Falcone
	Director, U.S. Army Ballistic Research Laboratory, Aberdeen Proving Ground, MD 21005-5066
1	ATTN: SLCBR-D, Dr. J. Frasier
1	SLCBR-TB, Dr. W. Kitchens
1	SLCBR-TB, Mr. Thomas Havel
1	SLCBR-TB, Dr. W. Gillich
1	SLCBR-TB, Mr. W. Gooch
1	SLCBR-TB, Dr. L. Magness
	Commander, U.S. Army Infantry Board, Fort Benning, GA 31905
2	ATTN: Materiel Division
	Commander, U.S. Army Aviation Systems Command, Aviation Research and Technology Activity, Aviation Applied Technology Directorate, Fort Eustis, VA 23604-5577
1	ATTN: SAVRT-TY-ASV, Mr. McAllister
1	SAVRT-TY-ASV, W. Swink
	Commander, U.S. Army Aviation Systems Command, 4300 Goodfellow Boulevard, St. Louis, MO 63120-1798
1	ATTN: AMSAV-GTD
1	AMSAV-E
1	AMCPEO-AV
	Commander, Rock Island Arsenal, Rock Island, IL 61299-6000
1	ATTN: SMCRI-SEM-T
	Naval Research Laboratory, Washington, DC 20375
1	ATTN: Dr. G. R. Yoder - Code 6384
	Chief of Naval Research, Arlington, VA 22217
1	ATTN: Code 471
	Director, Structural Mechanics Research, Office of Naval Research, 800 North Quincy Street, Arlington, VA 22203
1	ATTN: Dr. N. Perrone
1	Bruce MacDonald
1	Ralph Lud
	Commander, David Taylor Naval Ship Research and Development Center, Bethesda, MD 20084
1	ATTN: Rod Peterson - Code 1240
1	Herb Wolk - Code 1740.1
1	Richard Swanek - Code 1240
	Naval Air Development Center, Warminster, PA 18974
1	ATTN: Code 6062, Irv Shaffer
	Naval Air System Command, Department of the Navy, Washington, DC 20360
1	ATTN: AIR-03PAF
1	AIR-5164J, LT COL J. Sebolka
1	SEA-05M, Dr. Alex Kaznoff
1	SEA-05M8, LCDR W. M. Elger
1	SEA-05R 25, C. Zanis
	Naval Material Command, Washington, DC 20360
1	ATTN: MAT-0331
	Naval Research Laboratory, 455 Overlook Avenue, Washington, DC 20375
1	ATTN: T. W. Crooker
	Naval Surface Weapons Center, Dahlgren Laboratory, Dahlgren, VA 22448
1	ATTN: Code G-54, Mr. J. Hall
1	Code R-35, Dr. B. Smith
	Naval Weapons Center, China Lake, CA 93555
1	ATTN: Code 40701
1	Code 408
	Commander, U.S. Air Force Wright Aeronautical Laboratories, Wright-Patterson Air Force Base, OH 45433
1	ATTN: AFWAL/MLC
1	AFWAL/MLLP, D. M. Forney, Jr.
1	AFWAL/MLBC, Mr. Stanley Schulman
1	AFWAL/FIBC, Mr. L. G. Kelly
1	AFWAL/FIES, Mr. A. G. Kurtz
1	AFWAL/FIESD, Mr. A. Kurtz
	National Aeronautics and Space Administration, Marshall Space Flight Center, Huntsville, AL 35812
1	ATTN: R. J. Schwinghammer, EH01, Dir, M&P Lab
1	Mr. W. A. Wilson, EH41, Bldg. 4612
	Aeronautical Systems Division (AFSC), Wright-Patterson Air Force Base, OH 45433
1	ATTN: ASD/ENFEF, D. C. Wight
1	ASD/ENFTV, D. J. Wallick
1	ASD/XRHD, G. B. Bennett

No. of Copies	To
	McDonnell Douglas Helicopter Company, 5000 E. McDowell Road, Mesa, AZ 85205-9797
1	ATTN: Library, 2/T2124, D. K. Goss
1	Mr. A. Hirko
1	Mr. L. Soffa
	IIT Research Institute, 10 West 35th Street, Chicago, IL 60616
1	ATTN: K. McKee
	Kaman Aerospace Corporation, Old Winsor Road, Bloomfield, CT 06002
1	ATTN: H. E. Showalter
	Lockheed-California Company, A Division of Lockheed Aircraft Corporation, Burbank, CA 91503
1	ATTN: Technological Information Center, 84-40, U-35, A-1
	Vought Corporation, P.O. Box 5907, Dallas, TX 75232
1	ATTN: D. M. Reedy, 2-30110
	Martin Marietta Corporation, Orlando Division, P.O. Box 5837, Orlando, FL 32805
1	ATTN: Library, M. C. Griffith
	McDonnell Douglas Corporation, 3855 Lakewood Boulevard, Long Beach, CA 90846
1	ATTN: Technical Library, C1 290/36-84
	Northrop Corporation, Aircraft Division, 3901 W. Broadway, Hawthorne, CA 90250
1	ATTN: Mgr. Library Services, H. W. Jones
	Parker Hannifin Corporation, 14300 Alton Parkway, Irvine, CA 92718
1	ATTN: C. Beneker
	Armament Systems, Inc., 712-F North Valley, Anaheim, CA 92801
1	ATTN: J. Musch
	Beech Aircraft Corporation, 9709 E. Central Avenue, Wichita, KS 67206
1	ATTN: Engineering Library
	Bell Helicopter Company, A Textron Company, P.O. Box 482, Fort Worth, TX 76101
1	ATTN: J. R. Johnson
	Boeing Helicopters, P.O. Box 16858, Philadelphia, PA 19142-0858
1	ATTN: N. Caravasos, M/S P30-27
	Cessna Military, P.O. Box 7704, Wichita, KS 67277-7704
1	ATTN: Wallace
	Los Alamos National Laboratory, Los Alamos, NM 87545
1	ATTN: R. Mah
1	D. Sandstrom
1	W. Blumenthal
1	R. Barks
	Lawrence Livermore National Laboratory, P.O. Box 808, Livermore, CA 94550
1	ATTN: C. Cline
1	R. Landingham
	Aluminum Company of America, Alcoa Technical Center, Alcoa Center, PA 15069
1	ATTN: A. Becker
	CERCOM, Inc., 1960 Watson Way, Vista, CA 92083
1	ATTN: R. Palicka
	Ceradyne, Inc., 3169 Redhill, Costa Mesa, CA 92626
1	ATTN: E. Conabee
	Norton Co., 1 New Bond Street, Worcester, MA 01606
1	ATTN: R. Bart
	Coors Ceramics Co., 600 Ninth Street, Golden, CO 80401
1	ATTN: R. Paricio
	Carborundum Co., P.O. Box 1054, Niagara Falls, NY 14302
1	ATTN: J. Hinton
1	R. Palia

No. of Copies	To
	Air Force Armament Laboratory , Eglin Air Force Base, FL 32542
1	ATTN: AFATL/DLYA, V. D. Thornton
1	Mr. W. Dyess
	Air Force Flight Dynamics Laboratory, Wright-Patterson Air Force Base, OH 45433
1	ATTN: AFFDL/TST, Library
	NASA - Ames Research Center, Army Air Mobility Research and Development Laboratory, Mail Stop 207-5, Moffett Field, CA 94035
1	ATTN: SAVDL-AS-X, F. H. Immen
	U.S. Department of Commerce, National Institute of Standards and Technology, Gaithersburg, MD 20899
1	ATTN: Stephen M. Hsu, Chief, Ceramics Division, Institute for Materials Science and Engineering
	Director, Central Intelligence Agency, P.O. Box 1925, Washington, DC 20505
1	ATTN: OSWR-OSD, Ward Waltman
1	R. Gomez
1	J. Backofen
	U.S. Secret Service, Technical Development and Planning Division, 1301 L Street, N.W., Room 800, Washington, DC 20005
1	ATTN: John McCalla
	Office of Security, Department of State, Washington, DC 20520
1	ATTN: A/SY/OPS/T
	FMC Corporation, Ordnance Engineering Division, 1105 Coleman Avenue, San Jose, CA 95108
1	ATTN: Ron Musante
1	Tony Lee
1	Claude Braafladt
	General Dynamics, Land Systems Division, 38500 Mound Road, Mail Zone 4362029, Sterling Heights, MI 48310
1	ATTN: Mr. Richard Auyer
	United States Steel Corporation, Research Laboratory, Monroeville, PA 15146
1	ATTN: Dr. John M. Barsom
	L. Raymond & Associates, P.O. Box 7925, Newport Beach, CA 92658-7925
1	ATTN: Dr. L. Raymond
	Ingersoll Rand Oilfield Products Division, P.O. Box 1101, Pampa, TX 79065
1	ATTN: Mr. W. L. Hallerberg
	Lukens Steel Company, Coatesville, PA 19320
1	ATTN: Dr. E. G. Hamburg
	LTV Steel Corporation, 410 Oberlin Avenue SW, Massillon, OH 44646
1	ATTN: Mr. R. Sweeney
1	Mr. W. H. Brechtel
1	Mr. B. G. Hughes
	Boeing Advanced Systems, P.O. Box 3707, Seattle, WA 98124-2207
1	ATTN: R. J. Bristow, MS 33-04
1	W. Herlin, MS 33-04
	Sikorsky Aircraft, A Division of United Aircraft Corporation, Main Street, Stratford, CT 06601
1	ATTN: George Karas
	Teledyne CAE, 1330 Laskey Road, Toledo, OH 43697
1	ATTN: Librarian, M. Dowdell
	Fairchild Industries, Inc., Fairchild Republic Company, Conklin Street, Farmingdale, Long Island, NY 11735
1	ATTN: Engineering Library, G. A. Mauter
	Gruman Aerospace Corporation, South Oyster Bay Road, Bethpage, NY 11714
1	ATTN: Technical Information Center, J. Davis

No. of Copies	To
	Georgia Tech Research Institute, Georgia Institute of Technology, Atlanta, GA 30332
1	ATTN: K. V. Logan
	Southwest Research Institute, 6220 Culebra Rd., San Antonio, TX 78248
1	ATTN: C. Anderson
	University of California-San Diego, Dept. of Applied Mechanics & Engineering Sciences, La Jolla, CA 92093
1	ATTN: M. Meyers
	Dow Chemical Co., 1776 Building, Midland, MI 48674
1	ATTN: A. Hart
	Lanxide Corp., Tralee Industrial Park, Newark, DE 19711
1	ATTN: M. Newkirk
	General Sciences, Inc., 655 Gravers Road, Plymoth Meeting, PA 19462
1	ATTN: P. Zavitsanos

No. of Copies	To
	University of Dayton Research Institute, 300 College Park, Dayton, OH 45469
1	ATTN: S. Bless
1	N. Hecht
	SRI International, 333 Ravenswood Ave., Menlo Park, CA 94025
1	ATTN: D. Shockey
1	D. Curren
	Director, U.S. Army Materials Technology Laboratory, Watertown, MA 02172-0001
2	ATTN: SLCMT-TML, Library
1	Author

U.S. Army Materials Technology Laboratory
Watertown, Massachusetts 02172-0001
FRACTOGRAPHIC ANALYSIS OF LONG ROD PENETRATOR-ARMOR CERAMIC INTERACTIONS -
Michael J. Slavin

Technical Report MTL TR 89-93, October 1989, 15 pp- illus, D/A Project: 1L162105.AH84

AD_____
UNCLASSIFIED
UNLIMITED DISTRIBUTION

Key Words

Armor
Ceramic armor
Long rod penetrators

The stages of armor ceramic fracture and defeat mechanisms of the projectile have been well documented for small caliber rounds (.30 and .50 caliber ball and armor piercing). The recent ability to manufacture ceramic tiles capable of protecting vehicles against large caliber munitions has shifted research to incorporating these materials into ground systems. Though many studies are evaluating the relationship of processing, microstructure, and mechanical properties with ballistic performance, few programs have focused on the actual defeat mechanisms involved for these heavy threats. A program was initiated to evaluate the fracture of a ceramic target when impacted by a tungsten long rod penetrator (LRP). Following a conventional V50 test of a silicon carbide whisker-reinforced aluminum oxide, one target was serial sectioned from the rear. Very fine comminuted ceramic was painstakingly removed from the exit point of the LRP. Tungsten and steel particles were included in the ceramic powder. The steel was present from three sources: front plate penetration, back plate splash, and subsequent entry into the target of the pusher plate. A distinct transition from very fine ceramic rubble to large ceramic pieces with a boundary geometry identical to that of a fracture conoid was apparent. All metallic material uncovered was removed for fractographic evaluation. The tungsten particles had comminuted ceramic embedded in it. This fractured ceramic would have been subjected to the maximum stresses from the ballistic impact and would give specific details as to the fracture mode of the ceramic directly in front of the projectile. Scanning electron microscopy (SEM) showed that the defeat mechanisms of the LRP were ductile tearing and microerosion by the very fine comminuted ceramic. Both the alumina grains and silicon carbide whiskers showed signs of mixed failure modes (transgranular and intergranular).

U.S. Army Materials Technology Laboratory
Watertown, Massachusetts 02172-0001
FRACTOGRAPHIC ANALYSIS OF LONG ROD PENETRATOR-ARMOR CERAMIC INTERACTIONS -
Michael J. Slavin

Technical Report MTL TR 89-93, October 1989, 15 pp- illus, D/A Project: 1L162105.AH84

AD_____
UNCLASSIFIED
UNLIMITED DISTRIBUTION

Key Words

Armor
Ceramic armor
Long rod penetrators

The stages of armor ceramic fracture and defeat mechanisms of the projectile have been well documented for small caliber rounds (.30 and .50 caliber ball and armor piercing). The recent ability to manufacture ceramic tiles capable of protecting vehicles against large caliber munitions has shifted research to incorporating these materials into ground systems. Though many studies are evaluating the relationship of processing, microstructure, and mechanical properties with ballistic performance, few programs have focused on the actual defeat mechanisms involved for these heavy threats. A program was initiated to evaluate the fracture of a ceramic target when impacted by a tungsten long-rod penetrator (LRP). Following a conventional V50 test of a silicon carbide whisker-reinforced aluminum oxide, one target was serial sectioned from the rear. Very fine comminuted ceramic was painstakingly removed from the exit point of the LRP. Tungsten and steel particles were included in the ceramic powder. The steel was present from three sources: front plate penetration, back plate splash, and subsequent entry into the target of the pusher plate. A distinct transition from very fine ceramic rubble to large ceramic pieces with a boundary geometry identical to that of a fracture conoid was apparent. All metallic material uncovered was removed for fractographic evaluation. The tungsten particles had comminuted ceramic embedded in it. This fractured ceramic would have been subjected to the maximum stresses from the ballistic impact and would give specific details as to the fracture mode of the ceramic directly in front of the projectile. Scanning electron microscopy (SEM) showed that the defeat mechanisms of the LRP were ductile tearing and microerosion by the very fine comminuted ceramic. Both the alumina grains and silicon carbide whiskers showed signs of mixed failure modes (transgranular and intergranular).

U.S. Army Materials Technology Laboratory
Watertown, Massachusetts 02172-0001
FRACTOGRAPHIC ANALYSIS OF LONG ROD PENETRATOR-ARMOR CERAMIC INTERACTIONS -
Michael J. Slavin

Technical Report MTL TR 89-93, October 1989, 15 pp- illus, D/A Project: 1L162105.AH84

AD_____
UNCLASSIFIED
UNLIMITED DISTRIBUTION

Key Words

Armor
Ceramic armor
Long rod penetrators

The stages of armor ceramic fracture and defeat mechanisms of the projectile have been well documented for small caliber rounds (.30 and .50 caliber ball and armor piercing). The recent ability to manufacture ceramic tiles capable of protecting vehicles against large caliber munitions has shifted research to incorporating these materials into ground systems. Though many studies are evaluating the relationship of processing, microstructure, and mechanical properties with ballistic performance, few programs have focused on the actual defeat mechanisms involved for these heavy threats. A program was initiated to evaluate the fracture of a ceramic target when impacted by a tungsten long rod penetrator (LRP). Following a conventional V50 test of a silicon carbide whisker-reinforced aluminum oxide, one target was serial sectioned from the rear. Very fine comminuted ceramic was painstakingly removed from the exit point of the LRP. Tungsten and steel particles were included in the ceramic powder. The steel was present from three sources: front plate penetration, back plate splash, and subsequent entry into the target of the pusher plate. A distinct transition from very fine ceramic rubble to large ceramic pieces with a boundary geometry identical to that of a fracture conoid was apparent. All metallic material uncovered was removed for fractographic evaluation. The tungsten particles had comminuted ceramic embedded in it. This fractured ceramic would have been subjected to the maximum stresses from the ballistic impact and would give specific details as to the fracture mode of the ceramic directly in front of the projectile. Scanning electron microscopy (SEM) showed that the defeat mechanisms of the LRP were ductile tearing and microerosion by the very fine comminuted ceramic. Both the alumina grains and silicon carbide whiskers showed signs of mixed failure modes (transgranular and intergranular).

U.S. Army Materials Technology Laboratory
Watertown, Massachusetts 02172-0001
FRACTOGRAPHIC ANALYSIS OF LONG ROD PENETRATOR-ARMOR CERAMIC INTERACTIONS -
Michael J. Slavin

Technical Report MTL TR 89-93, October 1989, 15 pp- illus, D/A Project: 1L162105.AH84

AD_____
UNCLASSIFIED
UNLIMITED DISTRIBUTION

Key Words

Armor
Ceramic armor
Long rod penetrators

The stages of armor ceramic fracture and defeat mechanisms of the projectile have been well documented for small caliber rounds (.30 and .50 caliber ball and armor piercing). The recent ability to manufacture ceramic tiles capable of protecting vehicles against large caliber munitions has shifted research to incorporating these materials into ground systems. Though many studies are evaluating the relationship of processing, microstructure, and mechanical properties with ballistic performance, few programs have focused on the actual defeat mechanisms involved for these heavy threats. A program was initiated to evaluate the fracture of a ceramic target when impacted by a tungsten long-rod penetrator (LRP). Following a conventional V50 test of a silicon carbide whisker-reinforced aluminum oxide, one target was serial sectioned from the rear. Very fine comminuted ceramic was painstakingly removed from the exit point of the LRP. Tungsten and steel particles were included in the ceramic powder. The steel was present from three sources: front plate penetration, back plate splash, and subsequent entry into the target of the pusher plate. A distinct transition from very fine ceramic rubble to large ceramic pieces with a boundary geometry identical to that of a fracture conoid was apparent. All metallic material uncovered was removed for fractographic evaluation. The tungsten particles had comminuted ceramic embedded in it. This fractured ceramic would have been subjected to the maximum stresses from the ballistic impact and would give specific details as to the fracture mode of the ceramic directly in front of the projectile. Scanning electron microscopy (SEM) showed that the defeat mechanisms of the LRP were ductile tearing and microerosion by the very fine comminuted ceramic. Both the alumina grains and silicon carbide whiskers showed signs of mixed failure modes (transgranular and intergranular).